Numerical and Experimental Investigation of the K-regime of Boundary-Layer Transition

U. Rist
Institut für Aerodynamik und Gasdynamik, University of Stuttgart,
70550 Stuttgart, Germany
Y. S. Kachanov
Institute of Theoretical and Applied Mechanics, 630090 Novosibirsk, Russia

Summary

One particular case of K-type transition has been investigated using hot-wire measurements and spatial direct numerical simulation (*DNS*). Detailed quantitative comparisons of the results of both approaches showed very good agreement of the spatial disturbance development, the disturbance spectra, the instantaneous velocity traces, and the local frequency–spanwise-wave-number spectra. Indications for a direct generation of three-dimensional modes as higher harmonics of the fundamental modes were found. A closer look at the phase speeds of these modes, however, revealed that weak-nonlinear interactions are only initially appropriate to describe the flow, they fail when local events dominate, like, for example the formation of small-scale vortices in the boundary layer. The investigation of the later stages showed that the hot-wire 'spike'-signals are connected with small ring-like vortices.

1. Introduction

Since its discovery more than thirty years ago [1], the K-regime of boundary-layer transition has repeatedly attracted scientific attention due to its complicated nonlinear nature. Different, partly controversal, theoretical models to describe the initial disturbance development appeared during this period (cf. discussions in [1] – [5], for example). A verified numerical/experimental data base could help to evaluate such models and to more clearly identify the relevant mechanisms. Additional difficulties in exploring K-type transition are connected with the investigation of the 'late stage' which is dominated by the nonlinear, three-dimensional, and unsteady character of the disturbances. At present, there are only two feasible approaches for the investigation of this regime: the laboratory experiment, and the direct numerical simulation using the complete Navier-Stokes equations.

First comparisons of the experimental data obtained in [6, 7] with results of DNS carried out in [8, 9] proved to be very fruitful and showed very good quantitative agreement for the initial stage leading to the appearance of high-frequency

fluctuations called 'spikes'. Here we continue our combined theoretical and experimental studies of the K-breakdown with the purpose of verification of each others data and providing a more detailed data base for identification of the main physical mechanisms of this type of transition.

2. Experimental and numerical data base

The experiments were performed in Novosibirsk on a flat plate mounted in the ITAM low-turbulence wind tunnel running at a speed of $U_0 = 9.18m/s$. Disturbances were introduced by a vibrating ribbon driven at $f_1 = 96.4Hz$ ($F = 2\pi f_1 \nu / U_0^2 = 1.1 \cdot 10^{-4}$) and spanwise spacers with a periodicity of $\lambda_z = 25$mm in spanwise direction (z) placed at $x = 250$mm from the leading edge of the flat plate ($R = (U_0 \delta_1 / \nu)^{1/2} = 670$, where δ_1 is the displacement thickness). Covering the region from $x = 300$mm to $x = 700$mm, signals of the downstream velocity component u were registered using a single hot-wire probe. All time traces of the probe were recorded relative to the forcing current and the instantaneous 3-D flow field could thus be reconstructed from these recordings. The amplitude of the vibrating ribbon was adjusted so that the first spikes in the disturbance velocity traces occured at $x \approx 430$mm.

Several numerical simulations of these experiments have been performed in Stuttgart using the DNS-scheme originally developed by Fasel et al. [10], improved by Kloker et al. [11], and more recently by Kloker [12]. The scheme is based on spectral approximations of the spanwise z-coordinate by a truncated Fourier series ($-K \leq k \leq K$), and on fourth-order accurate finite-differences in downstream x- and wall-normal y-directions. Time integration of the discretized Navier-Stokes equations was performed by a fourth-order accurate Runge-Kutta scheme. Results of two such simulations are presented here: one on a 2674×121 grid using $K = 15$, and one using 1394×273 grid points and $K = 64$. The first integration domain extended over 10 δ_1 in y-direction[1], and from $x_0 = 188$mm to $x_N = 572$mm in downstream direction, the second extended over 11.4 δ_1 at $x_1 = 396$mm and until $x_N = 767$mm, with the 'artificial relaminarization zones'[11] in both simulations starting at $x = 502$mm, and $x = 663$mm, respectively.

Disturbances consisting of a large-amplitude 2-D TS-wave with nondimensional frequency $F = 1.1 \cdot 10^{-4}$ and a steady spanwise modulation with period $\lambda_z = 25$mm were introduced in the first simulation at $x = 250$mm using suction and blowing at the wall [10]. The disturbance amplitudes of the 2-D periodic forcing and of the 3-D steady mode at $x = 250$mm were chosen to closely match the u'-disturbance amplitudes at $x = 300$mm in the experiment. The second simulation was started using data and instantaneous boundary conditions at x_1 obtained from an earlier simulation.

3. Comparison of results

Detailed quantitative comparisons of the numerical results with the experimental measurements of the u-velocity component are presented both in physi-

[1] at inflow

cal space (section 3.1) and in spectral space after Fourier decomposition into frequency–spanwise-wave-number harmonics (section 3.2). A comparison of the 'late-stage' structures is presented in section 3.3. Data of the first simulation are shown, except were noted.

3.1 Comparison of disturbance amplitudes and phases

Amplitude and phase distributions of the u-velocity component versus x and y are directly compared in Figure 1. In addition to the *rms*-amplitudes of the disturbance signals, their harmonic content (after Fourier analysis) is also shown. A constant distance of $y = 4$mm from the flat plate was chosen in Figure 1a in order to demonstrate the good quantitative correlation of the data in the 'initial' and 'late-stage' of K-breakdown. The sudden increase of all amplitudes at the spanwise peak station quite clearly separates the two regimes. At the valley station, nothing similar is observed. A small branching of different curves in the DNS-data which is not observed in the experiments, indicates that the DNS-results using more spanwise modes (129 instead of 31) must be used for comparisons downstream of $x = 450$mm.

Amplitude and phase profiles for two x-stations, one before, and one after the sudden increase of the disturbance amplitudes are shown in Figures 1b and 1c, respectively. Although some differences appear in the comparison of the mean flow[2], especially in the outer part of the boundary layer, the mean-flow influence does not appear to be crucial for the disturbances, since their profiles agree qualitatively very well. Due to the rapid downstream amplification of the initial disturbances one could expect that a small raise of the upstream forcing amplitudes would lead to a quite perfect quantitative agreement of the numerical results with the experimental measurements.

The phase profiles in Figure 1b and c show the characteristic phase synchronization originally observed by Kachanov et al. [6] which is due to the 'spikes'. The phases are plotted relative to the instant of the passage of the 'spike'. Using this normalization, a small but throughout the boundary layer approximately constant phase shift of the numerical data relative to the measurements may be observed at $x = 450$mm. The shift amounts to $\phi_n \approx n \cdot 20^o$, where $n = f_n/f_0$, indicating that the 'spike' appears at a slightly different time (6% of the disturbance cycle). Such a good agreement of the numerical results with the measurements for $x = 450$mm was originally not expected from a simulation using 31 spanwise Fourier modes only.

The effect of increasing the number of spanwise modes in the computations is shown in the next figure together with a comparison of instantaneous 'peak'-disturbance profiles at $x = 450$mm. The results of the two data sets described in section 2 are shown in Figure 2a and b. Both agree quantitatively very well with the measurements in Figure 2c. As could be expected already from Figure 1, the agreement for the data using fewer spanwise modes is already rather good but it is improved using more spectral modes. We will nevertheless continue using

[2] At $x = 400$mm: $\delta_{1_{DNS}} = 1.52$mm, $\delta_{1_{Exp}} = 1.66$mm and at $x = 450$mm: $\delta_{1_{DNS}} = 1.66$mm, $\delta_{1_{Exp}} = 1.92$mm.

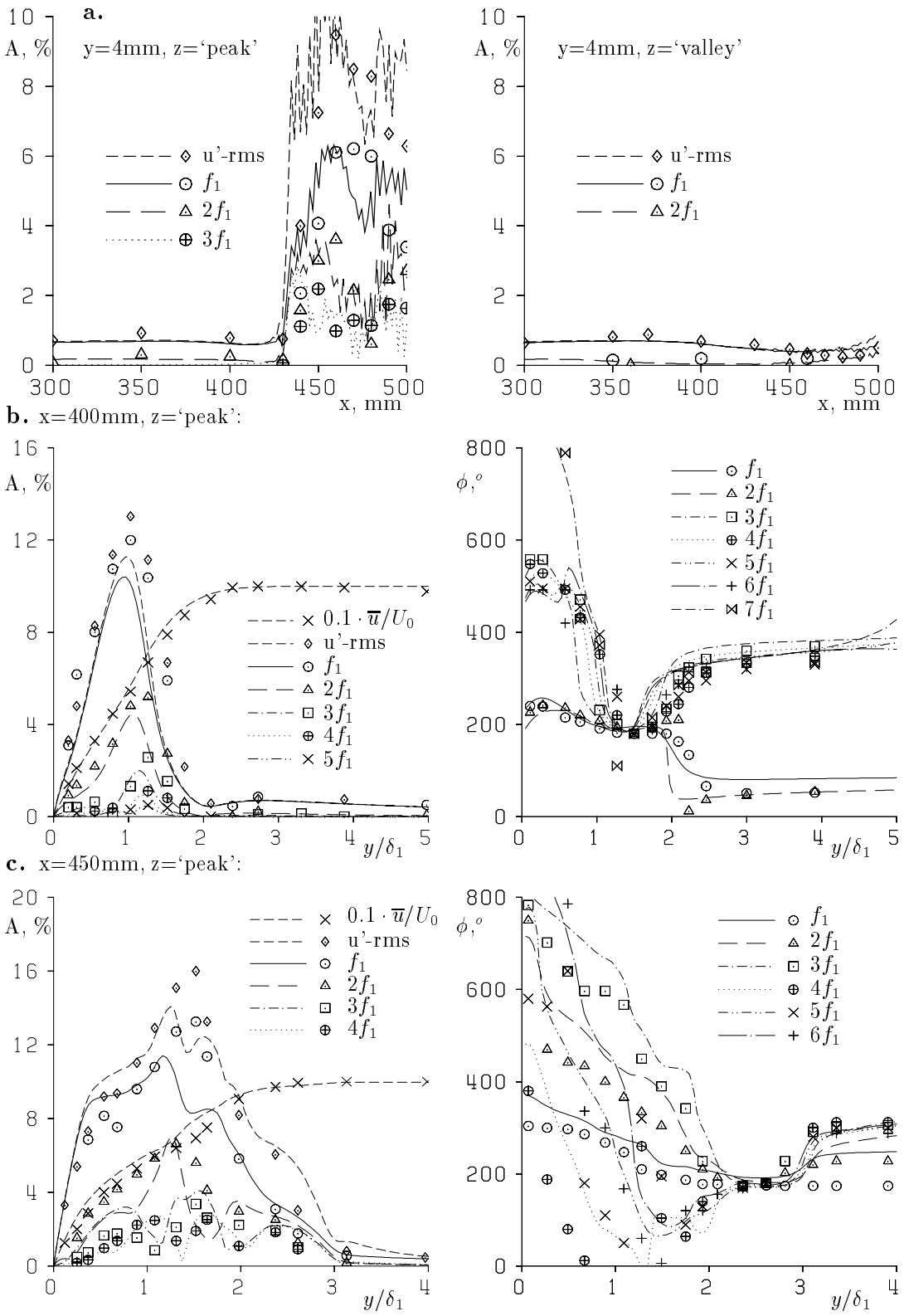

Figure 1: Comparison of mean flow ($\overline{u}$), u'-disturbance amplitudes (A), and phase profiles (ϕ). Lines = DNS, symbols = experimental measurements, f_1 = disturbance frequency.

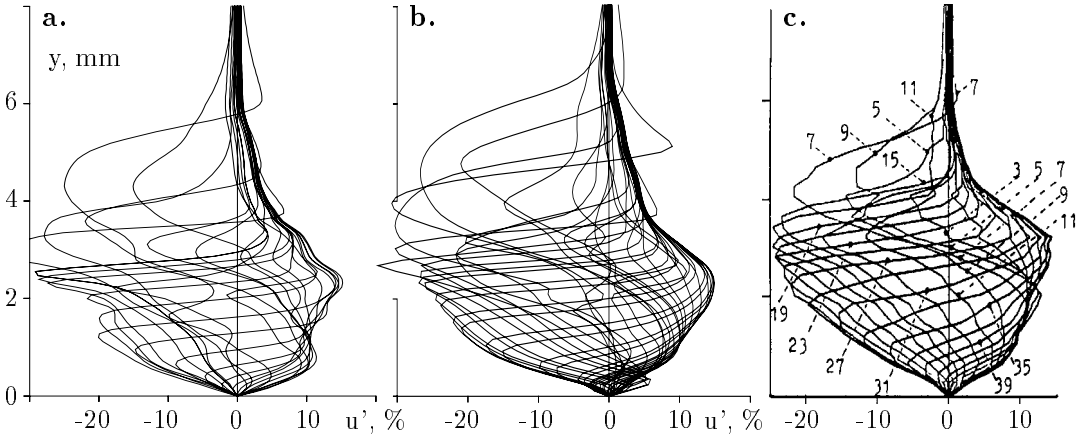

Figure 2: Comparison of instantaneous u'-amplitudes at $x = 450$mm, $z =$'peak'. **a.** Simulation using 31 spanwise modes (22 instants/period shown), **b.** simulation using 129 modes (28 instants/period), **c.** experiment (48 instants/period).

the first data set here, except for the comparison of the 'late-stage' structures in section 3.3.

3.2 Comparison of disturbance spectra

The study of the behavior of modes in frequency and frequency-wave-number-spectra as performed in [6, 7], for example gives information about possible weak-nonlinear disturbance interactions, as well as about the geometrical (shape) characteristics of the coherent structures observed at late stages of K-breakdown. The detailed comparison of the spectral amplitudes B defined by $u(x,y,z,t) = \sum_n \sum_k B_{n,k}(x,y) \cdot e^{i(nf_1 t + k\beta_0 z)} + c.c.$ at $y = 1$mm in Figure 3a illustrates the formation of spanwise and frequency higher harmonics with increasing x in very good quantitative agreement.

In a first step to isolate possible weak-nonlinear interactions between different (n,k)-modes, the approximate amplification rates $\kappa = B(x_1)/B(x_0)$ have been computed from Figure 3a and also compared in Figure 3b. Numerical and experimental results agree well for different frequencies and moderate values of the spanwise wave numbers. However, in contrast to the experimental data, the disturbances propagating at very high angles of inclination with respect to the flow direction grow much faster in the numerical simulation. One possible cause for this discrepancy might be due to less accurate amplitudes $B(x_0)$ in the experimental data when computing κ.

The strong increase of the amplification rates with the spanwise wave number indicates that the large-β modes are most probably just higher-harmonic disturbance components of the fundamental 3-D modes. Additional numerical computations showed that the large amplification rates just observed cannot be explained by parametric resonance of the 3-D modes with higher-harmonic 2-D modes, which is an idea originally stated in [7]. Test calculations using different initial amplitudes for these higher harmonics indicated that their downstream development (after an initial transient) is independent of the initial amplitude.

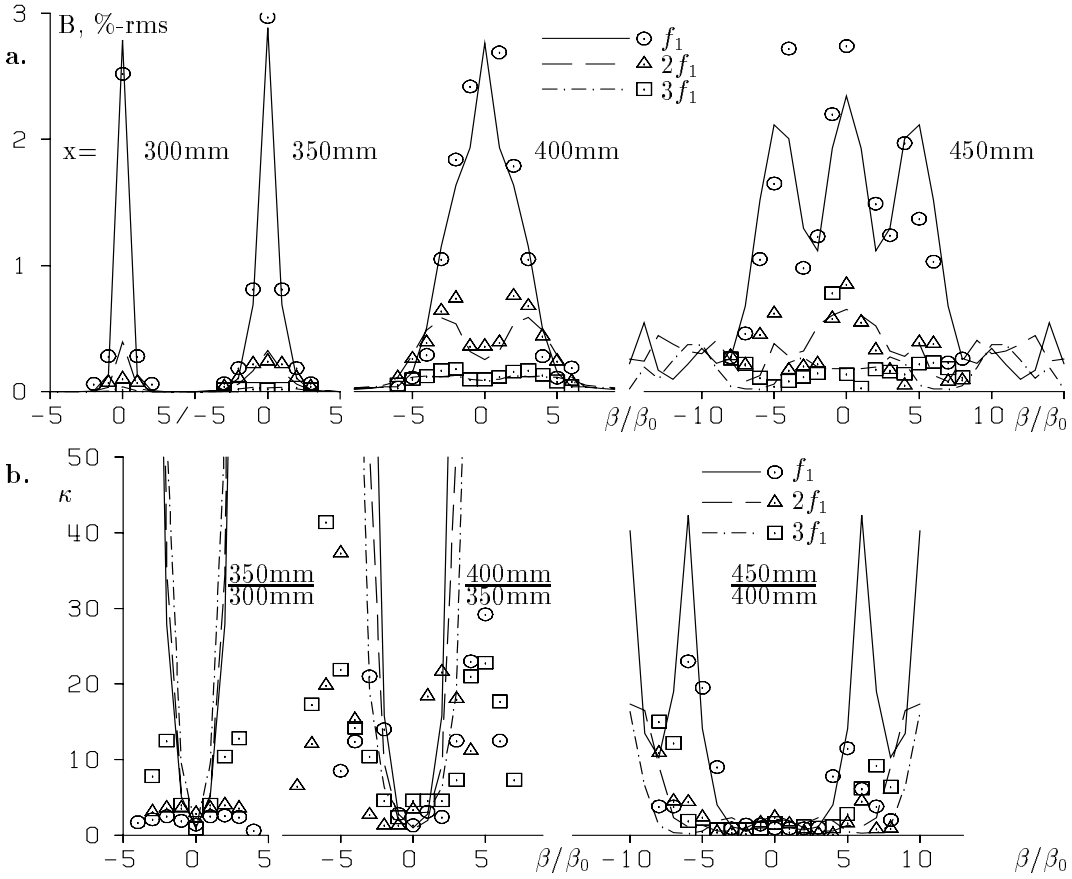

Figure 3: Comparison of spectral amplitudes B (**a.**) and amplification factors $\kappa = B(x_1)/B(x_0)$ (**b.**) vs. spanwise wave number at $y = 1$mm. Lines = DNS, symbols = experiments, spanwise wave number $\beta_0 = 2\pi/\lambda_z$, disturbance frequency f_1.

This also supports our interpretation.

Additional interesting spectral features are observed in the phase speeds of the (n,k)-modes in Figure 4. Initially (i.e., for small x), all modes have a 'wave-like' behavior, i.e., their phase speeds vs. y are constant and approximately equal, indicating a 'phase-lock' of higher harmonic modes with the fundamental modes. Also, one may correlate the amplitudes of single modes with the critical layer (y-position where $c_r = \overline{u}$): it appears that the nonlinearly generated higher harmonics do not necessarily have a maximum at y_{crit}. For larger x, however, c_r vs. y is no longer constant and each mode has a different phase speed outside of the boundary layer. In addition, the critical layer is at a y-position where no particularity is observed in the amplitude profiles. Around $y \approx 2$mm, instead, a new region appears where all modes have identical phase speed and rather large local disturbance amplitude of the higher harmonics. This is exactly the position where the 'spike' occurs. The 'spike' apparently belongs to a coherent structure that travels with its own speed. Weak-nonlinear wave interactions are most probably no longer appropriate to describe this behavior; local dynamics dominate, instead.

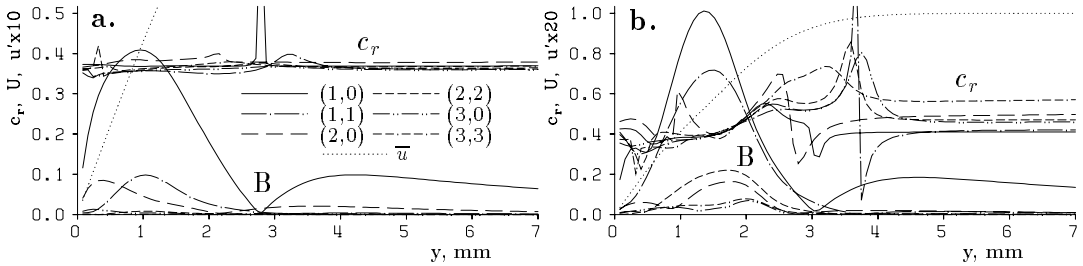

Figure 4: Comparison of phase speeds c_r with mean-velocity $\overline{u}$ and spectral amplitudes B for various frequency–spanwise-wave-number modes (n, k). **a.** $x = 350$mm, **b.** $x = 410$mm. (Simulation)

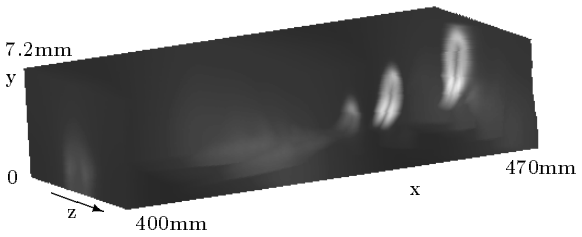

Figure 5: Volumetric perspective rendering of computed instantaneous 3-D pressure field. The grey scale used is proportional to $-p$, low-pressure regions therefore appear as light structures.

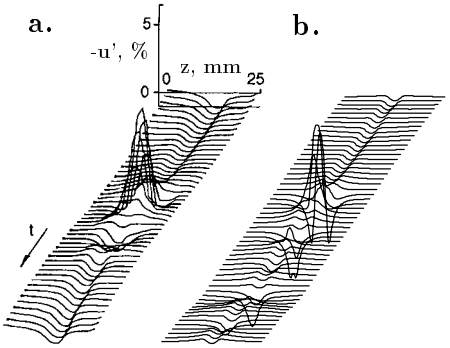

Figure 6: Comparison of 'spike'-signals vs. z and t at $x = 500$mm, $y = 8$mm. **a.** Experiment, **b.** Simulation.

3.3 Late-stage structures

Regarding the further development of spikes, including their multiplication and downstream convection in a soliton-like manner (for a discussion of these aspects see, e.g., [5, 13]), the comparison with the DNS gives also new insights: The spikes are connected with ring-like vortices snatching off from the downstream ends of Λ-vortices. This behavior can be seen in flow visualizations using particles, velocity, vorticity and pressure (cf. Figure 5). The typical scale of these new structures is of the same order as the boundary layer displacement thickness, and their shape, orientation and position within the boundary layer is very similar to those of so-called 'typical eddies' found in experiments by Falco [14] in the external part of developed turbulent flow. This indicates that the study of K-type transition is also important for the understanding of turbulent flows.

Using data of the latest finely resolved simulation, a detailed investigation of the final breakdown to turbulence is now possible. A first direct comparison of the 'spike'-amplitudes in the 'late stage' of K-breakdown is shown in Figure 6. Again, a very good quantitative agreement is observed using these new data.

4. Conclusions

By detailed quantitative comparisons of experimental measurements and results of direct numerical simulations, a validated data base has been generated that may be used for the validation of different theories, e.g., weakly nonlinear and

strongly nonlinear wave interactions, local inflectional instability, wave kinematics, soliton theory, etc. Evaluation of the 'late-stage' data has just begun, interesting new results may be expected.

Acknowledgements

The contributions of V.I. Borodulin, Novosibirsk to the experiments, and of M. Kloker, Stuttgart to the simulations are gratefully acknowledged.

References

[1] Klebanoff, P.S., Tidstrom, K.D. and Sargent, L.M.: The three-dimensional nature of boundary-layer instability, J. Fluid Mech. 12 (1962) 1-34.

[2] Craik, A.D.D.: Nonlinear evolution and breakdown in unstable boundary layers, J. Fluid Mech. 99 (1980) 247-265.

[3] Nishioka, M., Asai, M. and Iida S.: An experimental investigation of the secondary instability, *Laminar-Turbulent Transition* (eds. R. Eppler and H. Fasel), Springer, Berlin, Heidelberg (1980) 37-46.

[4] Borodulin, V.I. and Kachanov, Y.S.: Role of the mechanism of local secondary instability in K-breakdown of boundary layer. Izv. Sib. Otd. Akad. Nauk SSSR, Ser. Tekh. Nauk. 18 (1988) 65-77 (in Russian). (Transl. Soviet J. Appl. Phys. 3(2) (1989) 70-81.)

[5] Kachanov, Y.S.: Physical Mechanisms of laminar-boundary-layer transition, Ann. Rev. Fluid Mech. 26 (1994), 411-482.

[6] Kachanov, Y.S., Kozlov, V.V., Levchenko, V.Y. and Ramazanov, M.P.: On nature of K-breakdown of a laminar boundary-layer; new experimental data. *Laminar-Turbulent Transition* (ed. V.V. Kozlov), Springer, New York (1986) 61-73.

[7] Kachanov, Y.S.: On the resonant nature of the breakdown of a laminar boundary layer. J. Fluid Mech. 184 (1987) 43-74.

[8] Rist, U.: Numerische Untersuchung der räumlichen, dreidimensionalen Störungsentwicklung beim Grenzschichtumschlag. Dissertation Universität Stuttgart (1990).

[9] Rist, U. and Fasel, H.: Direct numerical simulation of controlled transition in a flat-plate boundary layer, J. Fluid Mech. (1985).

[10] Fasel, H.F., Rist, U. and Konzelmann, U.: Numerical investigation of the three-dimensional development in boundary-layer transition, AIAA J. 28 (1990) 29-37.

[11] Kloker, M., Konzelmann, U. and Fasel, H.: Outflow boundary conditions for spatial Navier-Stokes simulations of transitional boundary layers, AIAA J. 31 (1993) 620-628.

[12] Kloker, M.: Direkte Numerische Simulation des laminar-turbulenten Strömungsumschlages in einer stark verzögerten Grenzschicht, Dissertation Universität Stuttgart (1993).

[13] Kachanov, Y.S., Ryzhov, O.S. and Smith, F.T.: Formation of solitons in transitional boundary layers: theory and experiments. J. Fluid Mech. 251 (1993) 273-297.

[14] Falco, R.E.: Coherent motions in the outer region of turbulent boundary layers. Phys. Fluids Suppl. 20(10) (1977) S124-132.